Available online at www.sciencedirect.com

SCIENCE DIRECT®

Cement and Concrete Research 35 (2005) 1891–1899

Cement and Concrete Research

The squeezing test: a tool to identify firm cement-based material's rheological behaviour and evaluate their extrusion ability

Zahia Toutou[a,*], Nicolas Roussel[a], Christophe Lanos[b]

[a]Division Bétons et Composites Cimentaires, Point 41, Laboratoire Central des Ponts et Chaussées de Paris 58, Boulevard Lefebvre, 75738 Paris Cedex 15, France

[b]Institut National des Sciences Appliquées de Rennes, 20, avenue des Buttes des Coësmes, 35043 Rennes Cedex, France

Received 9 March 2004; accepted 7 September 2004

Abstract

The squeezing test is used in this paper as a rheological behaviour identification tool of cement-based materials in order to evaluate the extrusion ability. Experimental flow curves are obtained for firm cement pastes and fine sand firm mortars using two different compression speeds. These tested products may be considered as frictional plastic materials. Using the proposed testing method, two important aspects are discussed. On one hand, it is shown in this paper that the mortars bulk and apparent friction factors increase with sand addition proportion. On the other hand, cement paste's apparent yield shear stress increases at low compression speed because of fluid drainage through the granular skeleton and sample hardening. Some pictures obtained after squeezing test are used to illustrate this drainage phenomenon. Finally, some mortar mix design indications are proposed according to extrusion criteria based on rheological conditions.

Keywords: Squeezing test; Rheology; Permeability; Cement paste; Mortar

1. Introduction

Squeeze tests are often used in practice as a straightforward technique to determine the flow properties of highly concentrated suspensions such as molten polymers [1], ceramic pastes [2,3] or even hair gel [4]. Most of those materials behave as highly viscous or quasi-plastic fluids. Because of their high solid volume fraction, granular pastes such as firm cement pastes and firm mortars show frictional behaviour [5] that makes them highly sensitive to fluid drainage at slow flow velocities but high-pressure gradients [6]. Experimental evaluation of friction or drainage behaviour is not an easy problem. We propose to use squeeze flow to estimate characteristic parameters of the material's rheological and tribological behaviours. Such parameters ease the correlation adaptation between forming process and mix design. For example, friction and drainage phenomena involve high flow energy levels that could exceed some machine capacity during a shaping process, such as extrusion. In this paper, the squeezing test is used to study cement pastes and fine sand mortars flow. Different Water/Cement (W/C) and Sand/Cement (S/C) ratios are used to prepare the batches. Two squeezing velocities are studied: a "high" squeezing speed (v=5 mm/s) and a "low" one (v=0.5 mm/s).

For "high" squeezing speed, the material stays homogeneous through the test. In the case where no drainage occurs, the perfect yield plastic behaviour analytical solution is used to describe the experimental curves and allows the identification of the tested material plastic yield value. In the case where the drainage is instantaneous (high-permeability materials), a frictional plastic solution is used. Plastic yield stress, cohesion, bulk and apparent friction factors are identified and analyzed. Those parameters are directly linked to suitable extrudability conditions. On one hand, yield stresses and friction factors must not induce high extrusion pressure that can exceed the extruder capacity. On the other hand, a sufficient material yield value is needed for

* Corresponding author. Tel.: +33 1 40 43 51 65; fax: +33 1 40 43 54 93.
E-mail address: zahia.toutou@lcpc.fr (Z. Toutou).

0008-8846/$ - see front matter © 2004 Elsevier Ltd. All rights reserved.
doi:10.1016/j.cemconres.2004.09.007

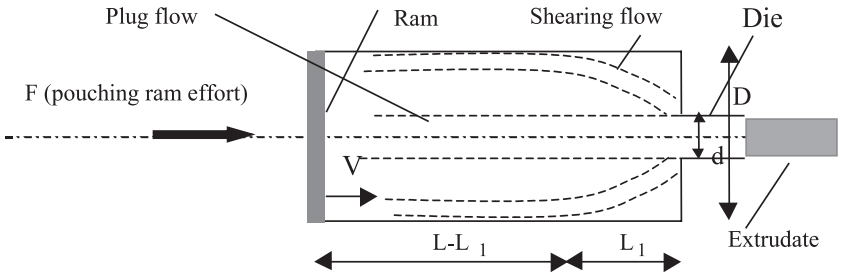

Fig. 1. Ceramic paste extrusion flow typology: a plug flow for L-L_1 length and a shearing and convergent flow for L_1 length.

the extruded products to retain the shape fixed by the die geometry.

For the "low" compression speed in the case of low permeability materials, drainage occurs through the test and heterogeneity appears. At the end of the "slow" squeezing test, the sample centre is drier compared to the one obtained from the "rapid" test. The influence of compression velocity, W/C and S/C parameters on the obtained experimental curves is discussed. In addition, qualitative interpretation of the drainage phenomenon shows that the cement paste composition modifies the dry zone radius. This phenomenon has to be mastered in order to avoid blockage and dead zones apparition during the extrusion process.

2. Extruded materials behaviour

Firm cement pastes or mortars used in extrusion process may be described by two different types of plastic behaviours: the perfect plastic body, following Von Mises criterion [7] and the plastic stress hardening or frictional plastic behaviour following Drucker–Prager criterion [8].

2.1. Perfect plastic behaviour

The perfect plastic behaviour involves the plastic yield value K_i. This type of behaviour appears when the flow is undrained. At a wall interface, the flow may be sticking or sliding according to the interface roughness.

2.2. Frictional plastic behaviour

If it is assumed that the Drucker–Prager criterion is suitable to describe yielded frictional behaviour, the modified yield stress K_{if} depends on the local pressure p via an internal friction parameter f.

$$K_{if} = K_i + f.p \tag{1}$$

At the wall interface, the coulomb criterion is fulfilled and an apparent friction factor f_z is defined, linking the shear stress τ and the total normal stress σ.

$$f_z = \frac{\tau}{\sigma + \dfrac{K_i}{f}} \tag{2}$$

On a general point of view, the undrained frictional behaviour involves two global parameters: the apparent cohesion C and the global bulk friction factor $\tan(\varphi)$ similar to the ones used to study dry granular materials. It could be reminded here that such an approach is suitable only for particularly firm cement pastes or mortars.

During an extrusion process, extrusion quality requires a balance between processing and material rheological properties. The material must be soft enough to flow into and through the extrusion die and yet be rigid enough to retain the shape fixed by the die geometry on one hand. The shape retention ability is linked to the cohesion parameter C or the plastic yield value K_i depending on the material behaviour. On the other hand, in case of perfect plastic materials, Mortreui et al. [8] and Chan and Baird [1] show that extrusion pressure is only linked to the material yield stress K_i and the section reduction ratio d/D (Fig. 1). They assume a yielded frictional behaviour for their studied materials and propose the extrusion flow typology shown on Fig. 1. However, in case of non-yielded frictional materials (i.e., the friction is speed dependant) or when drainage phenomena occur, a stress component linked to frictional energy dissipation must be added when studying the global extrusion pressure. This component increases when the frictional zone (L-L_1 length shown on Fig. 1) increases. Thus, the barrel length, the apparent and bulk friction factors f_z and $\tan(\varphi)$ directly influence this component. The frictional property is often coupled with interstitial fluid drainage in case of cement-based materials, as it will be seen in the following sections. In addition, the apparent friction factor can be responsible of flaws apparition on the extrudates exiting the die due to alternation of sticking

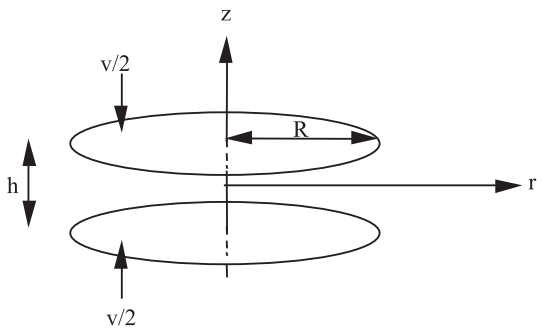

Fig. 2. Squeezing test geometry.

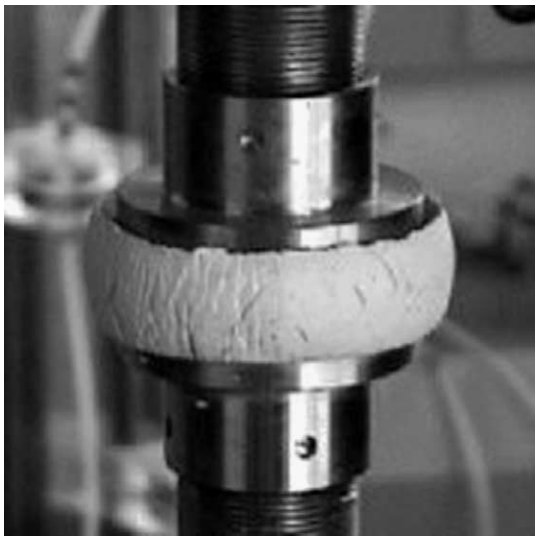

Fig. 3. Clay paste sample compression. The picture is taken before squeezing test starts.

and sliding flows. Ait Mokhtar et al. [9], when studying clay pastes extrusion, proposes 20 kPa as a limit value of the cohesion parameter C regarding deflexion of pieces during handling after extrusion. Finally, all of these identified rheological parameters can be introduced in an extrusion flow law such as Benbow [10] model to simulate the material extrusion flow. Firm cement-based materials extrusion ability optimization can then be obtained by mix optimization method based on all of these parameters vs. the die geometry change. This will become possible by using the equivalence between the dynamic, cinematic and geometric parameters of extrusion flow and squeezing test [1,11,12].

3. Description of the squeezing test

In this paper, the chosen squeezing test is a simple compression test carried out using an INSTRON-4507 Press on cylindrical samples with reduced slenderness. The apparatus consists in two coaxial circular and parallel plates without any rotation. The upper disc can be displaced at controlled constant velocity, while the lower one is maintained stationary. The sample squeezing between the two plates induces an essentially radial flow. R is the plate radius, h the sample height, F the compression load applied on the plates and v the constant compression speed (Fig. 2). Since the compression machine used here is designed to study rather solid materials, the maximum force value is 200 kN and the uncertainty is ± 0.005 kN. The gap between the plates is measured using a LVDT strain gauge with 100-mm maximum stroke and ± 0.06-mm accuracy. The tested material fills permanently the area between the plates (Fig. 3). The plate's roughness is also a test parameter. Use of rough plates imposes a sticking flow. The no-slip boundary condition is fulfilled. On the other hand, in the case of rectified plates, the material can slip along the solid surface. In this work, only rough plates are used.

4. Theoretical analysis

4.1. Perfect plastic behaviour

In the case of perfect plastic flow, a global equilibrium method is used by Ref. [13] in order to take into account the shearing layer influence on the pressure field inside the sample. Flow is assumed to occur everywhere in the sample and the Von Mises plasticity criterion is fulfilled at any point in the tested volume. The sample height is assumed to be small enough to consider that the total radial stress does not depend on the axial component z. In the case of a sticking flow, the shear stress at the plate/sample interface is equal to the plastic yield value K_i. This approach assumes, in the case of a sticking flow, the existence of a thin shearing layer at the interface where a strong velocity gradient appears as shown on Fig. 4.

The pressure gradient then writes:

$$\frac{dp}{dr} = -2\frac{K_i}{h} \tag{3}$$

The pressure at $r=R$ is assumed to be equal to the atmospheric pressure, which is taken as the reference pressure. The pressure at the interface becomes:

$$p(r, z = h/2) = \frac{2K_i}{h}(R - r) \tag{4}$$

The compression load could then be integrated from the pressure on the plates, which is itself integrated from the pressure gradient, but there has been disagreement about the stress or pressure boundary conditions at the edge of sample

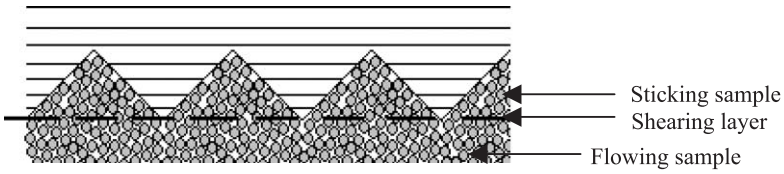

Fig. 4. Thin shearing layer at the interface in the case of rough plates. Scale between grains and interface roughness on this figure is not in accordance with the real sizes.

(r=R) [14]. The compression force is then calculated from the energy dissipation and writes [13]:

$$F = -\frac{2\pi K_i R^2}{\sqrt{3}} - \frac{2\pi K_i R^3}{3h} \tag{5}$$

The first part of Eq. (5) is linked to the energy dissipation in the extensional flow zone. The second part of Eq. (5) is linked to the shearing condition on the plates. These two dissipated energies are similar to the ones that can be found during an extrusion process.

The compression load does not depend on the compression rate as is to be expected from an analysis based upon plasticity theory. Reduced parameters are used to plot the test results (Lanos and Doustens [14]): the reduced compression load $F^*=-Fh/\pi R^3$ and the geometrical ratio h/R. The model then predicts:

$$F^* = \frac{2K_i}{\sqrt{3}}\left(\frac{h}{R}\right) + \frac{2K_i}{3} \tag{6}$$

$F^*(h/R)$ appears as a linear function of the geometrical ratio. Moreover, F^* is directly linked to the energy dissipation rate in the sample and as such does not depend on the plate radius as shown in Roussel and Lanos [13]. The experimental curves are fitted by linear regression in (h/R, F^*) coordinate. The slope and initial value of the experimental answer are used to assess K_i.

4.2. Drucker–Prager plastic behaviour

In the case of concentrated cement pastes and mortars, the compression speed may have an influence on the compression force because of consolidation phenomena. The non-homogeneous stress in the sample generates in the liquid phase an interstitial pressure gradient that is the engine of a liquid migration. During very slow flow, the centre of the sample becomes drier with a consequent increase in the plastic yield stress. An Eulerian description of this two-phase flow was written by Ref. [6] in the particular case of perfect plastic fluids submitted to slow squeezing. The local behaviour may still be considered as a perfect plastic but the plastic yield stress is a function of the local water content. The test results exploitation becomes far more difficult as it will be shown in Section 4. Without going here further in this analysis, it should be noted that this drainage phenomenon emphasises the frictional granular component of the tested fresh material behaviour. Lanos and Doustens [14] propose an approximate analytical model of plastic frictional fluid flow. This modelling is based on the fact that the total pressure gradient is comparable to the effective pressure gradient in the draining solid mass that occurs quasi instantaneous. The model is based on the Drucker–Prager [15] plastic criterion and on apparent Coulomb friction law [16].

The chosen plastic criterion writes:

$$K_{if} = K_i + fp \tag{7}$$

With f the internal friction parameter and p the local pressure.

Using the same extensional flow assumption as in Section 3, the shear stress τ_{rz} on the plate surfaces is equal to K_{if} and the normal stress σ_z is equal to:

$$\sigma_z = \frac{2}{\sqrt{3}}K_{if} + p \tag{8}$$

Eqs. (3), (7) and (8) give:

$$\left.\begin{array}{l} \dfrac{\partial \sigma_z}{\partial_r} = \left(\dfrac{2}{\sqrt{3}}f + 1\right)\dfrac{\partial p}{\partial r} \\ \dfrac{\sigma_z - \dfrac{2}{\sqrt{3}}K_i}{\dfrac{2}{\sqrt{3}}f + 1} = p \end{array}\right\} \Rightarrow \frac{\partial \sigma_z}{\partial r} = -\frac{2f}{h}\left(\sigma_z + \frac{K_i}{f}\right) \tag{9}$$

Regarding Coulomb behaviour, an apparent friction factor on plate f_z is introduced writing:

$$f_z = \frac{\tau_{rz}}{\sigma_z + \dfrac{K_i}{f}} = \frac{f}{\dfrac{2}{\sqrt{3}}f + 1} \tag{10}$$

Eq. (7) is integrated. The average compression stress P is then calculated. At the boundary (r=R), σ_z is equal to P_0, this term takes into account the effect of K_i and external pressure condition on the solution.

$$P = \frac{F}{\pi R^2} = P_0\frac{h^2}{2f^2R^2}\exp(2fR/h) - P_0\frac{h}{fR}(1 + h/2fR) \tag{11}$$

This equation converges to perfect plastic solution [Eq. (5)] when f tends towards 0 and K_{if} towards K_i. Based on the (fP) vs. P experimental curve, a reverse method is used to find P_0 and f. The calculation principle consists in identifying for each point of the $F^*(h/R)$ response curves f and P_0 parameters values that satisfy Eq. (11) and its first derivate according to h/R. If the (fP) vs. P evolution is not linear the Drucker–Prager criterion is not suitable to describe the tested material.

Two characteristic parameters are estimated from the linear regression of the (fP) vs. (P) curve: the apparent cohesion C corresponding to the initial fP value of the linear regression and the global bulk friction factor, tan(φ) linked to the slope of linear regression and interpreted as the apparent friction factor f_z. These two parameters are calculated using two couples [P_1, $fP(P_1)$] and [P_2, $fP(P_2)$], of $fP(P)$ curves, following:

$$C = fP(P_1) - \frac{fP(P_2) - fP(P_1)}{P_2 - P_1}P_1 \tag{12}$$

$$tg\varphi = \frac{fP(P_2) - fP(P_1)}{P_2 - P_1}\Bigg/\left(1 + 2.\frac{fP(P_2) - fP(P_1)}{P_2 - P_1}\Bigg/\sqrt{3}\right) \tag{13}$$

5. Experimental results

5.1. Tested materials

Cement pastes were prepared using 52.5 CEM1 Lafarge cement (Saint-Pierre-La-Cour, France) and 30% of cement mass substituted by filler fines additions. Three fillers were used: silica fume 0.1 μm maximum particle diameter, volcanic rock finely crushed 15 μm maximum particle diameter and amorphous crushed quartz 10 μm maximum particle diameter. The paste was obtained by using water and WRA (Sika plastiment 22S). Mortars were obtained by adding fine sand (0/0.630 mm) to the cement pastes. The different mixture compositions are given in Table 1.

5.2. Mixing procedure and test parameters

A planetary Hobart Kitchen mixer is used. It provides sufficiently high shear rates for small batches. First, dry ingredients are mixed for about 2 min at the lowest mixer rpm setting. Then, water and plasticizer are added. Once the dry ingredients are moistened, a higher rotation speed is applied for 5 min. Cylindrical samples (40 mm height and 40 mm radius) are then moulded using either ramming in the case of firm mixtures or vibration (50 Hz) in case of soft ones. The squeezing test plate radius is R=40 mm (equal to sample's radius) and only serrated surface plates (1 mm serration height) are used in this study. The tests are carried out using two compression speeds: v=0.5 mm/s for the slow test and v=5 mm/s for the rapid test.

5.3. F* vs. h/R experimental curves

The results show two kinds of $F^*(h/R)$ curves. The transition between these two test answer types is linked to the test compression speed.

Table 1
Tested material compositions and specimen identification

Specimen ID	Water/ cement	Plasticizer/ cement	Solid vol. fraction (%)	Sand vol. fraction (%)
Cement pastes				
CP # 22-0	0.22	0	68.8	0
CP # 22-06	0.22	0.006	68.3	0
CP # 22-08	0.22	0.008	68.2	0
CP # 22-1	0.22	0.01	68.0	0
CP # 25-0	0.25	0.0	66.0	0
CP # 25-1	0.25	0.01	65.2	0
CP # 27-0	0.27	0	64.3	0
CP # 30-1	0.30	0.01	61.1	0
Mortars				
Mor # 01	0.25	0.01	75.1	28.5
Mor # 02	0.25	0.01	76.8	33.2
Mor # 03	0.30	0.01	73.5	31.8
Mor # 04	0.30	0.01	77.1	41.1

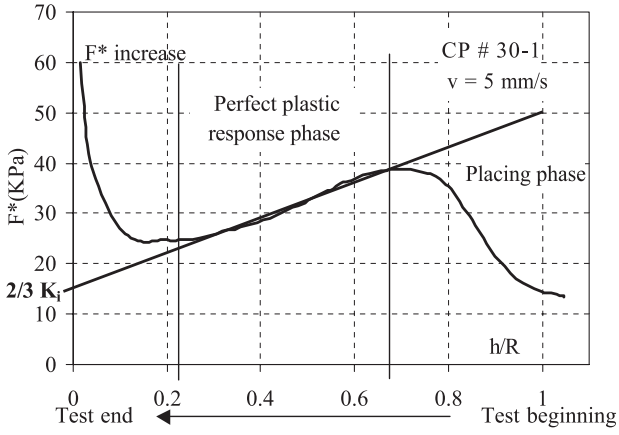

Fig. 5. Typical experimental granular plastic material $F^*(h/R)$ response curve. Case of CP # 30-1 Mix. The bold line represents the theoretical purely plastic answer.

5.3.1. "*High*" *compression speed tests: perfect plastic behaviour*

This kind of response is obtained for some cement paste formula such as PC # 30-1 and PC # 27-0 (Fig. 5) and all the tested mortar formula (Fig. 6). The global response curves show at the beginning of the test, a placing phase for h/R>0.75, followed by a linear phase for 0.5<h/R<0.75 and finally a phase consisting in a very high F^* increase for h/R<0.5 (Fig. 5). The material flow is assumed to be established only after the placing phase, which is not exploited in this study.

We can see on Figs. 5 and 6 that the plastic response is obtained only for short ranges of h/R values. Broadly, the range of h/R values corresponding to this response decreases when the solid volume fraction increases. The plastic yield values are calculated from these h/R value ranges using Eq. (4) experimental fitting (Table 2).

In case of cement pastes, the plastic yield value decreases when the ratio W/C increases. In case of mortars for the same ratio W/C, the plastic yield value decreases when the

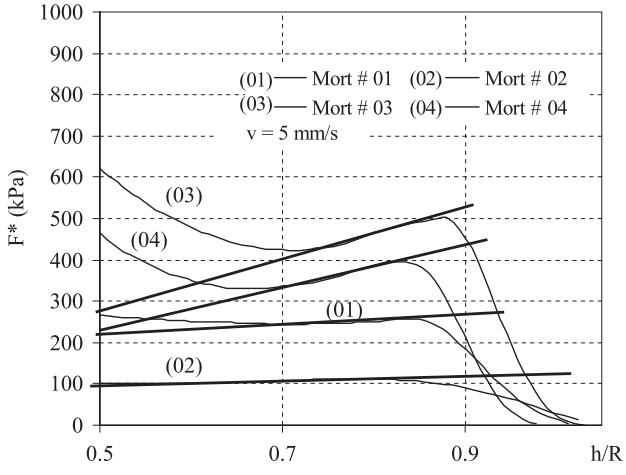

Fig. 6. Tested mortars $F^*(h/R)$ experimental results. Bold lines represent the theoretical purely plastic answer.

Table 2
Calculated plastic yield values—high compression speed test

Specimen ID	Solid volume fraction (%)	W/C	K_i (kPa)
CP # 27-0	64.3	0.27	91
CP # 30-1	61.1	0.30	20
Mort # 01	75.1	0.25	244
Mort # 02	76.8	0.25	145
Mort # 03	73.5	0.30	95
Mort # 04	77.1	0.30	55

S/C ratio increases. This last result may be explained by the fact that the physicochemical links between cement particles are reduced when the sand volume fraction increases. However, in case of a high sand volume fraction the plastic yield value may be increases because of the sand frictional component that will be added to the cement particles links [5].

For low h/R values, $F^*(h/R)$ increases when h/R decreases. This property is linked to the intergranular friction of the consolidated material. The material behaviour changes for this range of h/R values. In this range, a frictional plastic model has to be used in order to identify the material frictional properties as shown in the following section.

5.3.2. "High" compression speed tests and low h/R values: frictional plastic behaviour

For "high" compression speed test and low h/R values or for the slow compression test, the global effort F^* increases continuously when h/R decreases. Using the solution written in Section 3, the pseudo-friction yield stress (fP) evolution vs. the average compression stress P is obtained. The curve shapes are quite linear, which validates the use of our model (Figs. 7 and 8). As we can see on Fig. 8, the friction model seems more valid in case of mortars.

At "low" speed test, a fluid drainage occurs. This will be examined in the next section. In this case, the sample

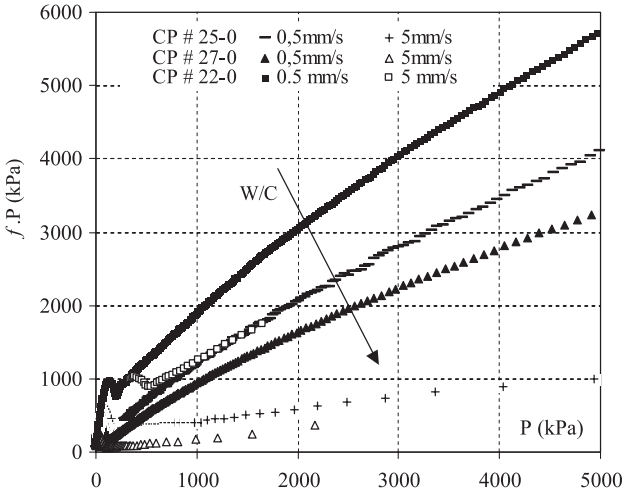

Fig. 7. Cement pastes (fP) vs. (P) evolution.

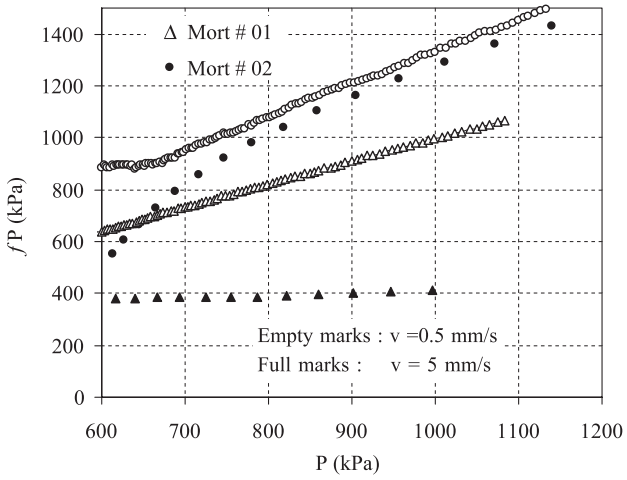

Fig. 8. Mortars (fP) vs. (P) evolution.

becomes non-homogeneous during the test so that the results cannot be directly exploitable. The analysis focuses here on the materials features obtained from the rapid squeezing test only. The cohesion, bulk and apparent friction factors are identified (Table 3) using linear regression on curve part linked to h/R data superior to 0.2. For all the tested formula, apparent friction factor is greater than the bulk one. For a same W/C ratio, the two friction factors decrease when the ratio PL/C increases in case of cement pastes or when the sand volume fraction decreases in case of mortars. The same tendency is obtained for the cohesion parameter and the values are generally higher than K_i (Tables 2 and 3). Conforming to these results, an optimisation of the two W/C and PL/C formulation ratio values must be first done in order to get adequate friction and cohesion parameters that permit material extrusion in the given extrusion conditions (extruder capacity, die geometry etc.). For all the studied materials, we can conclude that the obtained cohesion values are higher than

Table 3
Tested material's frictional properties calculated for $0.5<P<5$ MPa and $v=5$ mm/s

	Solid vol. fraction (%)	C (kPa)	f_z	$tg\varphi$
Cement paste ID				
CP # 22-0	68.8	545	0.46	0.40
CP # 22-06	68.3	482	0.42	0.36
CP # 22-08	68.2	291	0.40	0.37
CP #22-1	68.0	409	0.41	0.35
CP # 25-0	66.0	254	0.22	0.13
CP # 25-1	65.2	82	0.30	0.31
CP # 27-0	64.3	225	0.13	0.06
CP # 30-1	61.1	53	0.12	0.11
Mortars ID				
Mor # 01	28.5	254	0.39	0.31
Mor # 02	33.2	313	0.48	0.45
Mor # 03	31.8	54	0.28	0.20
Mor # 04	41.1	365	0.49	0.47

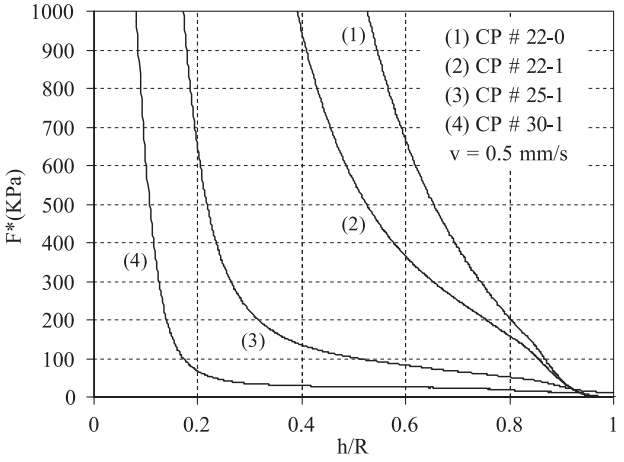

Fig. 9. Cement pastes F^* vs. h/R curves.

the limit value corresponding to extrudate good shape retention (K_i or C>20 kPa).

5.3.3. "Low" compression speed tests and high h/R values: drainage effect

For slow compression tests and at high h/R ($h/R \approx 1$) values, a recorded very high global effort F^* increase may be noticed (Figs. 9 and 10). This response can be linked to the intergranular friction amplified by a local solid volume fraction evolution. An interstitial fluid drainage through the granular skeleton occurs.

In this case, a non-homogeneous flow is expected during the test and the plastic frictional behaviour response analysis, written in Section 3, has to include the drainage phenomenon taking into account a distinction between skeleton pressure and interstitial fluid pressure. Roussel [6] used a simplified method to describe the fluid drainage phenomenon through the solid skeleton in case of clay pastes submitted to low compression speed squeezing test. A plastic frictional behaviour model is used in case of non-homogeneous flow but the used local plastic yield value in Eq. (1) depends on the test history (pressure history). It isolates in drainage phenomenon solution in two parts: a diffusion part and a transport one. The first one is linked to the material permeability whereas the second one is linked to the imposed changing shape of the sample. The lower is the material permeability greater is the diffusion phenom-

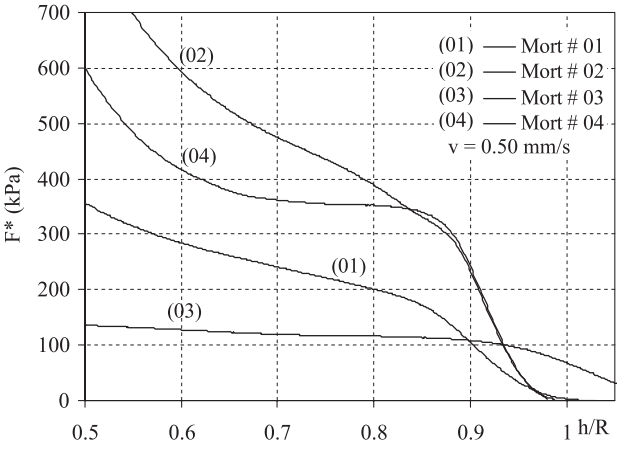

Fig. 10. Mortars F^* vs. h/R curves.

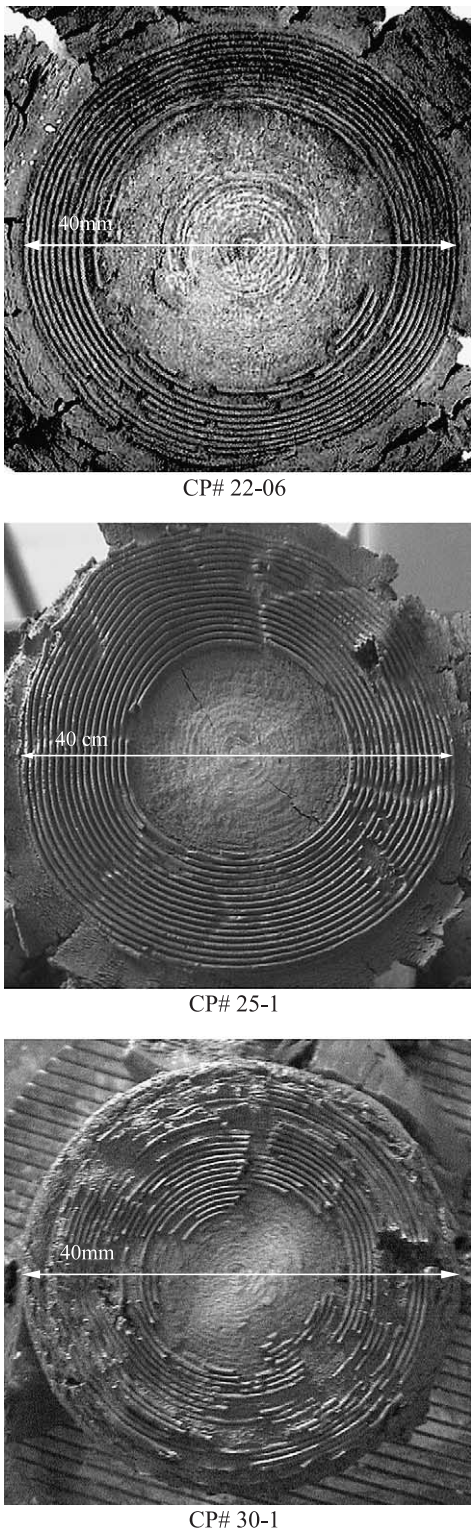

Fig. 11. Cement paste sample photos obtained at the end of slow squeezing test (v=0.5 mm/s).

enon. Conversely, the solution approaches the solution of a transport equation for materials with high permeability. The diffusion and transport phenomena are complementary.

This drainage solution cannot be used to describe cement based pastes or mortars drainage property, as its adaptation to the case of frictional behaviour is too complex. At this stage of the study, we can just say that, in such materials, the drainage occurs essentially by "transport" because of their relatively high permeability. Hence, the drainage occurs quasi instantly showing a face of migration between two zones of water content values: a zone where the water content tends towards a limit value (water content that cannot extracted mechanically) and a zone where the water content evolves in time, because of high permeability. The experimental measurement of the tested sample water content appears technically difficult in case of cement-based materials (setting phenomenon). However, it is possible to note visually the consequences of the drainage on the tested samples. At the end of the test, and for low compression speeds, the samples show a dried central zone where the paste colour has changed clear grey. The pictures presented on Fig. 11 show examples of cement pastes samples obtained at the end of low compression speed tests (v=0.5 mm/s).

It should be noted that at the lower compression speed, W/C and/or PL/C ratios are proportional to the dried zone radius (Fig. 12). We also noted that this clear grey colour disappears at few minutes later and the sample centre returns to its initial colour. The water content gradient generated by slow compression is the engine of a water content rebalancing once the test is finished.

During the extrusion process local drainage phenomenon can induce a large increase in extrusion pressure and can collapse the extrusion or induces a non-homogeneous shape. In all parts of extruder, the flow speed must be sufficient and the extruder jacket must be waterproof. A limit speed value corresponding to the drainage apparition was assessed by the analysis proposed by Ref. [17], when studying mud with large water content. It will be interesting in future work to adapt this approach to cement based pastes and mortars study.

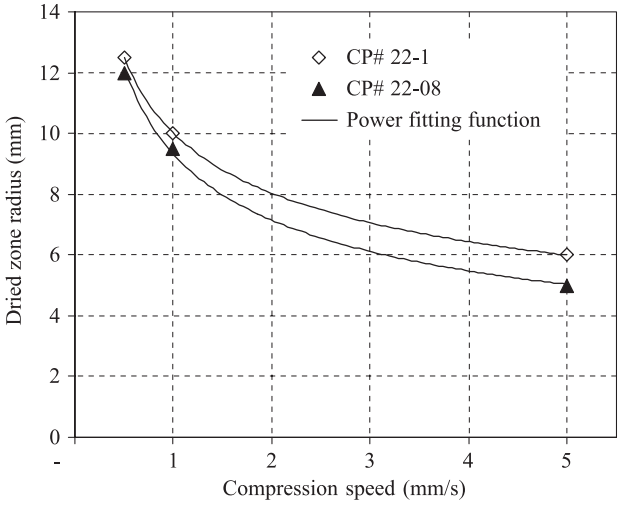

Fig. 12. Dried zone radius vs. compression speed test.

6. Conclusion

It is important to know in which conditions cement based materials can be shaped by extrusion. This study introduced the squeezing test as an extrusion-ability-identifying tool. This is possible because of the existing similitude between the extrusion flow and the induced squeezing test flow. The squeezing test is used to identify some rheological parameters that control both the material/tool interaction and the extrudate quality. From a general point of view, extrusion quality requires a balance between processing and material rheological properties. The material must be soft enough to flow into and through the extrusion die and yet be rigid enough to retain the shape given by the die geometry. The shape retention is linked to the material cohesion whereas the softness is assessed by the bulk plastic yield stress. The external extrudate aspect (no flaws, no wrenching, no curls etc.) is linked to the material/tool interaction according to whether the material behaves as sliding, sticking or frictional material against a metal interface.

It is shown in this study that firm cement pastes and firm fine sand mortars rheological behaviours are speed dependant. For high compression speeds, these materials show homogeneous and cohesive plastic behaviour. The experimental responses are modelled using a perfect plastic solution according to Von Mises criterion allowing the identification of the material plastic yield value. For low compression speeds, the tested materials show a drained and frictional plastic behaviour. In this case, a model based on Coulomb frictional law and Drucker–Prager plastic criterion is used to describe the experimental curves. Tested materials cohesion, apparent and bulk friction factors are identified. The results confirm the occurring fluid drainage throw the granular skeleton. In addition, sample's photos that show dried central zone induced by a water migration from the sample centre to its borders illustrated this phenomenon.

Finally, before extruding firm cement based materials, a judicious optimisation of the batches composition must be first determined in order to get adequate rheological parameters that allow the material extrusion in the given extrusion conditions (extruder capacity, pressure, extrusion velocity, die geometry etc.).

Notations

C	Cohesion [Pa]
F	Compression force [N]
F^*	Reduced compression load defined by $Fh/\pi R^2$ [Pa]
f	Coulomb apparent friction parameter
f_z	Material apparent friction factor
h	Plate separation or sample's height [m]

K_i Plastic yield value defined according to Von Mises criterion [Pa]
K_{if} Modified plastic yield value in case of a Drucker–Prager criterion [Pa]
P Local pressure [Pa]
P_0 Pressure at the boundary R=0 of the plate
P Average compression stress [Pa]
PL/C WRA cement ratio (by mass)
R Plate radius [m]
S/C Sand cement ratio (by mass)
σ_z Normal stress [Pa]
τ_{rz} Shear stress at the plate surfaces [Pa]
$tg\varphi$ Material bulk friction factor
V Compression speed [m/s]
W/C Water cement ratio (by mass)

References

[1] T.W. Chan, D.G. Baird, An evaluation of a squeeze flow rheometer for the rheological characterisation of a filled polymer with a yield stress, Rheol. Acta 41 (2002) 245–256.
[2] A. Ait mokhtar, Mise au point d'essais de laboratoire pour la caractérisation de l'étude de l'extrudabilité de pâtes argileuses. Thèse de doctorat INSA de Rennes, 1993.
[3] C. Lanos, Identification of the rheological behaviour of mineral pastes by using compression test, Proc. XIIIth International Congress of Rheology, vol. 2, British Society of Rheology, Cambridge, 2000, pp. 415–417.
[4] P. Estellé, C. Lanos, Y. Mélinge, C. Servais, Le test de compression simple: mise en œuvre sur un analyseur de texture et exploitation en présence de fluides viscoélastiques, Rhéologie 3 (2003) 39–45.
[5] S. Mansoutre, P. Colombet, H. Van Damme, Water retention and granular rheological behaviour of fresh C3S paste as function of concentration, Cem. Concr. Res. 29 (9) (1999) 1441–1453.
[6] N. Roussel, C. Lanos, Y. Mélinge, Introduced heterogeneity in saturated flowing granular media, Powder Technol. 138 (2003) 68–72.
[7] R. Von Mises, Mechanik der Plastichen Formänderung von Kristallen, Z. Angew. Math. Mech. (1928) 6.
[8] F.X. Mortreuil, C. Lanos, M. Laquerbe, A model for recombining clay paste plastic flow in dies, XIIIth International Congress on Rheology, vol. 3, British Society of Rheology, Cambridge, 2000, pp. 400–402.
[9] A. Ait Mokhtar, C. Lanos, A. Doustens, M. Laquerbe, Evaluation de l'aptitude à l'extrusion d'un fluide épais, Ind. Céram. Verr. 897 (1994) 632–637.
[10] J.J. Benbow, The dependence of output rate on die shape during catalyst extrusion, Chem. Eng. Sci. 26 (1971) 1467–1473.
[11] Z. Toutou, C. Lanos, Y. Mélinge, The use of the squeezing test–extrusion flow similitude to identify cement based materials extrudability domain, The XIVth International Congress on Rheology COEX Convention Center Seoul Korea August 22–27, 2004.
[12] Z. Toutou, Rhéologie et formulation des géosuspensions concentrées: évaluation des conditions d'extrudabilité, Thèse Doctorale INSA de Rennes, 2002.
[13] N. Roussel, C. Lanos, Plastic fluid flow identification using a simple squeezing test, Appl. Rheol. 13 (3) (2003) 132–141.
[14] C. Lanos, A. Doustens, Rhéométrie des écoulements entre plateaux parallèles: réflexions, Eur. J. Mech. Eng. 39 (2) (1994) 77–89.
[15] D.C. Drucker, W. Prager, Soil mechanics and plastic analysis or limit design, Q. Appl. Math. 10 (1952).
[16] J.H. Atkinson, P.L. Bransby, The Mechanics of Soils. Introduction to Critical State Soil Mechanics, McGraw-hill book (UK), Limited Maidenhead Berkshire England, 1978.
[17] M. Chaouche, F. Chaari, G. Racineaux, A. Poitou, Comportement de fluides pâteux en écoulement d'écrasement, Rhéologie 3 (2003) 46–52.